INDUCTION MACHINE MODELLING WITH DYNAMIC ECCENTRICITY FAULT USING FMM AND PERMEANCE APPROACH

S. Hamdani
Laboratoire des systèmes électriques et industriels, USTHB Université des sciences et de technologies Houari Boumedien BP 32 El Alia 16111 Bab Ezzouar ; Alger ; Algérie;E-mail: shamdani@usthb.dz

O. Touhami R. Ibtiouen
Laboratoire de Recherche en Electrotechnique, Ecole Nationale Polytechnique, BP 182 El Harrach 16200, Algerie,

M. Fadel
Laboratoire Plasma et Conversion d'Energie; ENSEEIHT, 2 rue Charles Camichel
BP 7122, F-31071 Toulouse cedex 7, France.

M. Hassan
Elec. Power & Machines Dept., Cairo University , Giza, Egypt

S. Gadoue
Department of Electrical Engineering, Alexandria University, Alexandria, 21544, Egypt

Abstract: *This paper deals with modelling the induction machine with dynamic eccentricity fault. The machine inductances are calculated using the magneto motive force and the air gap permeance approach taking into consideration the space harmonics effect. First, the magnitude and the form of the obtained inductances in presence of dynamic eccentricity are discussed and compared to those of the healthy machine. Next, these inductances are introduced in the general induction machine model obtained using the magnetically coupled circuits approach. Simulation results illustrate the induction machine performances for the healthy and the faulty cases. The Fast Fourier Transform (FFT) of the steady state stator current obtained by simulation is performed to detect specific components that identify the fault appearance in the machine. The detection of these components is easier when the motor is supplied from a sinusoidal voltage than when supplied from a Pulse Width Modulation (PWM) inverter.*

Key words: *Dynamic Eccentricity, Induction Machine, Permeance, Magneto Motive Force*

1. Introduction

Among electrical machines, induction motors are the most widely used in industry because of their rugged configuration, low cost, and versatility. With their great contributions, induction motors are considered the workhorse of industry. Because of natural aging processes and other factors in practical applications, induction motors are subject to various faults, such as rotor faults. These faults can be induced by electrical failures such as a bar defect or bar breakage or mechanical failures such as rotor eccentricity. The first fault occurs due to thermal stresses, hot spots, or fatigue stresses during transient operations such as start-up, especially in large motors. A broken bar changes the machine developed torque significantly and can seriously affect the safe and consistent operation of electric machines [1].

The second type of rotor faults is related to air gap eccentricity. This fault is a common effect related to a range of mechanical problems in induction motors such as load unbalance or shaft misalignment. Long-term load unbalance can damage the bearings and the bearing housing and influence air gap symmetry. The research in detecting the air gap eccentricity of induction motors began in the last century. Existing detection schemes are classified according to the type of monitoring parameters. Examples of monitoring parameters include torque, flux, vibration signal, and stator current. Depending on whether the minimum air gap is spatially fixed or not, air gap eccentricity is described as being either static or dynamic. For static eccentricity, the rotor shifts from its normal position at the center of the stator and rotates around its own center. For dynamic eccentricity, the rotor shifts from its normal position, but still rotates around the center of the stator [2- 4].

Induction motor modeling with dynamic eccentricity using the winding function approach has been widely investigated [5-8]. The frequency components generated by dynamic eccentricity are explained analytically in [5]. Using the rotating field approach, authors confirm the existence of specific frequency components around the fundamental, caused by the dynamic air gap eccentricity. The interactions between the dynamic eccentricity and the inherent static eccentricity are also illustrated using an adequate

mathematical model of the induction machine. In this model, the calculation of inductances is performed by the modified winding function approach.

The Authors in [6] used the coupled magnetic circuit approaches to model the induction machine under dynamic eccentricity. The inductances are calculated directly from the geometry and layout of the machine using the turn and winding function approach. Simulation results are presented in this paper to show the behavior of the induction machine under this fault. In [7], authors use the extension of winding function approach to calculate and evaluate machine inductances for a nonuniform air gap. In this approach, the modified winding function is defined as the difference between the turn function for uniform air gap and its average in one period. Using this approach, it was confirmed that the mutual inductances calculated from stator and rotor are not the same. The Modified Winding Function Approach (MWFA) is also used in [8]. Compared to [7], the axial variable (z) was introduced in addition to the polar variable (φ, r) for inductances calculation.

Although, in all the papers discussed above and also in other papers [9-11], the winding function approach has been used, the analytical expression of the self and mutual inductances of the induction machine has never presented. For that reason, this paper aims to introduce the analytical formulation of these inductances using the Magneto Motive Force (MMF) and the permeance function approach considering space harmonics. First, the Fourier series decomposition of the stator and the rotor MMFs will be presented. These MMFs are multiplied by the permeance function and integrated cross a surface to produce the flux. Inductances are obtained by dividing the flux linkage by the current. The magnitude and the form of these inductances in presence of dynamic eccentricity are discussed and compared to those of the healthy machine. The calculated inductances are introduced in the general induction machine model obtained using the magnetically coupled circuits approach. Simulation results illustrating the induction machine performances for the healthy the faulty cases are presented. Also, the Fast Fourier Transform FFT of the steady state stator current is performed to detect any specific component which identifies the fault appearance in the machine.

The paper is organized as follow: section 2 presents the dynamic model of the induction machine, while section 3 describes the methodology used for inductances calculation and illustrates analytical formulations of these inductances. Simulation results are discussed and analysed in section 4.

2. Dynamic Model of the Induction Machine

The induction machine is modelled as a set of coupled circuits consisting of the individual coils of the stator windings and the loops of the rotor formed by rotor bars and end-ring segments. The effect of space harmonics of the MMF and the air-gap permeance is incorporated in the model. The model parameters are evaluated from the geometry and the winding layout of the machine. With many assumptions to neglect saturation and slot effects, this model reduces the complexity of coding and computations dramatically. According to coupled magnetic circuits approach, it is possible to establish the voltage equations of stator and rotor loops as [12]:

$$\begin{cases} V_s = R_s.I_s + \dfrac{d\phi_s}{dt} \\ 0 = R_r.I_r + \dfrac{d\phi_r}{dt} \\ \phi_s = L_s I_s + M_{sr} I_r \\ \phi_r = L_r.I_r + M_{rs}.I_s \end{cases} \quad (1)$$

where V_s is the stator voltage, I_s and I_r are the stator and the rotor currents, ϕ_s and ϕ_r are the stator and the rotor flux linkage, R_s and L_s are a 3 by 3 stator resistance and inductance matrix, R_r and L_r are a (Nr+1)x(Nr+1) rotor resistance and inductance matrix. M_{sr} is a 3 by N_r+1 matrix consisting of mutual inductances between stator coils and the rotor loops plus the end ring, where M_{rs} is a N_r+1 by 3 matrix consisting of mutual inductances between rotor loops and the stator coils. The mechanical equation of motion depends upon the characteristics of the load. It is assumed here that the torque which opposes that produced by the machine consists of the inertial torque, the friction torque and the external load torque which are explicitly known. In this case the mechanical equation of motion can be simply given as:

$$\frac{d\omega_r}{dt} = \frac{1}{I_{nert}}\left(C_{em} - K_f.\omega_r - C_L\right) \quad (2)$$

where C_L is the load torque and K_f is the friction constant. The electromagnetic torque produced by the machine C_{em} can be obtained from the magnetic co-energy equation as: [13]:

$$C_{em} = \left[\frac{dW_{co}}{d\theta_r}\right]_{(I_s, I_r constants)} \quad (3)$$

In a linear magnetic system, the co-energy is equal to the stored magnetic energy:

$$W_{co} = \frac{1}{2}\left(I_s^t.L_s.I_s + I_s^t.L_{sr}.I_r + I_r^t.L_{rs}.I_s + I_r^t.L_r.I_r\right) \quad (4)$$

3. Inductances Calculation

It is well known that a successful simulation of an induction motors requires a precise calculation of all motor inductances. As it was discussed in section 1, many papers use the MWFA for inductances

calculation. Inductances which change with rotor position such as stator-rotor mutual inductance (M_{sr}) must be evaluated at every simulation step. In the discussed papers, discrete curves of mutual inductances and their derivatives versus rotor angular position are pre-computed and stored in luck-up table. Within the iteration loop, the inductances are obtained by linear interpolation. This additional operation increases simulation time. In this paper, analytical expression of induction machine with dynamic eccentricity fault will be presented using the MMF and the air-gap permeance approach. The resulting inductances expressions are less complicated and can be introduced in the simulation script for calculation at every step without the need for interpolation. Moreover, since mutual inductances derivative are also needed, their expression can be easily obtained and used for torque calculation.

3.1. Self and mutual inductances of stator phases

The self inductance L_{si} of any stator phase i (i=1, 2, 3) can be given by the following equation:

$$L_{si} = \frac{\phi_{si}}{i_{si}} \tag{5}$$

where ϕ_{si} is the flux linked to this phase generated only by the current i_{si} following the same phase. Due to the high permeability of stator and rotor steel and the short length of the air gap relative to the inside stator diameter, the magnetic field essentially exist only in the air gap and tend to be radial in direction, even with an eccentric rotor [3,4].

At first, let us consider the flux linkages of a single coil of stator winding which is located between φ_{s1} and φ_{s2} in the stator reference frame. In this case, the flux is determined by performing a surface integral over the open surface of the single coil:

$$\phi_{sie}(\varphi_s) = r.L.\int_{\varphi_{s1}}^{\varphi_{s2}} F_{si}(\varphi_s).\lambda(\varphi_s,\theta_r).d\varphi_s \tag{6}$$

where r is the average air gap radius, L is the core length. $F_{si}(\varphi_s)$ is the stator phase FMM and $\lambda(\varphi_s,\theta_r)$ is the air-gap permeance function, they can be given respectively by:

$$F_s(\varphi_s) = \sum_{n=1}^{\infty} \frac{2.N_{sp}.i_s}{\pi.n.p} K_b(n.p).cos(n.p.\varphi_s) \tag{7}$$

$$\lambda(\varphi_s,\theta_r) = \lambda_0.\left(1 + 2.\sum_{n=1}^{\infty} \lambda_n.cos(k.(\varphi_s - \theta_r))\right) \tag{8}$$

$$\begin{cases} \lambda_0 = \dfrac{\mu_0}{\varepsilon_0.\sqrt{1-\delta_d^2}} \\ \lambda_n = \left(\dfrac{1-\sqrt{1-\delta_d^2}}{\delta_d}\right)^n \end{cases} \tag{9}$$

where $K_b(n.p)$ is the winding factor of the space harmonic of rank n given by :

$$K_b(n.p) = sin\left(\frac{n.p.\tau}{2}\right).\frac{sin\left(N_{es}.n.p.\dfrac{\pi}{N_s}\right)}{sin\left(n.p.\dfrac{\pi}{N_s}\right)} \quad \text{.....} \tag{10}$$

where N_{sp} is the number of series coils per phase, ε_0 is the mean air-gap length, μ_0 is the air magnetic permeability and δ_d is the dynamic eccentricity degree. However, the flux linked to the stator phase can be obtained by adding the flux linked to all the coils which constitute this phase:

$$\phi_{si} = (n_e.r.L).\left[\sum_{m1=0}^{Nes-1}\sum_{m2=0}^{p-1}\int_{\beta_1}^{\beta_2} F_{si}(\varphi_s).\lambda(\varphi_s,\theta_r).d\varphi_s\right] \tag{11}$$

where:

$$\begin{cases} \beta_1 = -\dfrac{\tau}{2} - (N_{es}-1)\dfrac{\pi}{N_s} + m_1.\dfrac{2.\pi}{N_s} + m_2.\dfrac{2.\pi}{p} \\ \beta_2 = \dfrac{\tau}{2} - (N_{es}-1)\dfrac{\pi}{N_s} + m_1.\dfrac{2.\pi}{N_s} + m_2.\dfrac{2.\pi}{p} \end{cases} \tag{12}$$

Taking into account equation (12) and substituting $F_{si}(\varphi_s)$ and $\lambda(\varphi_s, \theta_r)$ by their expressions given respectively by (7) and (8), the stator self inductance can be obtained after calculation and simplification by the following relation:

$$(L_{si})_{de} = (L_{si})_{de1} + (L_{si})_{de2} \tag{13}$$

where $(L_{si})_{de1}$ and $(L_{si})_{de2}$ are given by (14) and (15) respectively.

$$\begin{aligned} (L_{si})_{de1} &= \frac{4.\mu_0.r.L.N_{sp}^2}{\pi.p^2.\varepsilon_0.\sqrt{1-\delta_d^2}}\left(\sum_{n=1}^{\infty}\left(\frac{K_b(n.p)}{n}\right)^2\right) \\ &= \frac{L_{s0}}{\sqrt{1-\delta_d^2}}.\sum_{n=1}^{\infty}\left(\frac{K_b(n.p)}{n}\right)^2 = \frac{(L_{si})_{healthy}}{\sqrt{1-\delta_d^2}} \end{aligned} \tag{14}$$

$$(L_{sisi})_{de2} = \frac{L_{s0}}{\sqrt{1-\delta_d^2}}.\sum_{n=1}^{\infty}\frac{K_b(n.p)}{n}.\sum_{k=1}^{\infty}(A_k + B_k).cos(k\theta_r) \tag{15}$$

with:

$$\begin{cases} A_k = \lambda_k.\left(\dfrac{K_b(n.p+k)}{(n.p+k)}.\sum_{m_2=0}^{p-1} cos\left((n.p+k).m_2.\dfrac{2.\pi}{p}\right)\right) \\ B_k = \lambda_k.\left(\dfrac{K_b(n.p-k)}{(n.p-k)}.\sum_{m_2=0}^{p-1} cos\left((n.p-k).m_2.\dfrac{2.\pi}{p}\right)\right) \end{cases} \quad (16)$$

Similarly, the expressions for mutual inductance L_{sisj} between two stator phases i and j can be derived using the same procedure and introducing only the phase angle (φ_{sisj} =(j-i).2π/3) between these phases. Therefore, the following expression can be obtained:

$$(L_{sisj})_{de} = (L_{sisj})_{de1} + (L_{sisj})_{de2} \quad (17)$$

where $(L_{sisj})_{de1}$ and $(L_{sisj})_{de2}$ are given by (18) and (19) respectively

$$\begin{aligned}(L_{sisj})_{de1} &= \frac{L_{s0}}{\sqrt{1-\delta_d^2}}\sum_{n=1}^{\infty}\left(\frac{K_b(n.p)}{n}\right)^2.cos(n.p.\varphi_{sisj}) \\ &= \frac{(L_{sisj})_{healthy}}{\sqrt{1-\delta_d^2}}\end{aligned} \quad (18)$$

$$(L_{sisj})_{de2} = \frac{L_{s0}}{\sqrt{1-\delta_d^2}}.\sum_{n=1}^{\infty}\frac{K_b(n.p)}{n}.\sum_{k=1}^{\infty}\begin{pmatrix} A_k.cos(k\theta_r + n.p.\varphi_{sisj}) \\ + B_k.cos(k\theta_r - n.p.\varphi_{sisj})\end{pmatrix} \quad (19)$$

It can be noted from the above expressions that in presence of dynamic eccentricity, the self and mutual inductances of the stator phases are function of the rotor position. Therefore, this fact should be taken into account during the calculation of the electromagnetic torque. To illustrate this variation, Figure 1 shows the self and the mutual inductance between the first and the second stator phase for a healthy machine and a machine with δ_d=70% of dynamic eccentricity. It can be noted that the amplitude of these inductances increases with the degree of dynamic eccentricity.

3.2. Self and mutual inductances of rotor loops

The rotor can be considered as equivalent to a m-phase two layer winding. A turn (loop) is formed by the conductors in the top layer of one slot and the bottom layer of the adjacent slot. The current i_r following in the turn is the current in the end ring between the two slots. The number of phases in such a winding would be m=Nr/p where Nr expresses the number of rotor bars. The phase shift between the currents in two adjacent turns is $2\pi/m = 2\pi.p/Nr$ since the rotor bars are spaced by the angle α_r=2.π/N_r [9]. Using this approach, the FMM F_{rj} of the j^{th} loop can be written as:

$$F_{rj}(\varphi_r) = \sum_{n=1}^{\infty}\frac{2.i_r}{\pi.n}sin\left(n.\frac{\alpha_r}{2}\right)cos(n.\varphi_r) \quad (20)$$

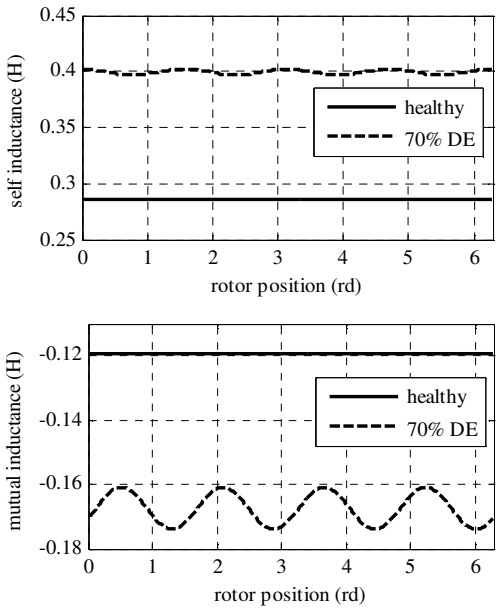

Fig. 1 Self and mutual inductances of the stator phase

Hence, the self inductance for any rotor loop can be calculated as:

$$(L_{rj})_{de} = r.L.\int_{-\frac{\alpha_r}{2}}^{\frac{\alpha_r}{2}} F_{rj}(\varphi_r).\lambda(\varphi_r).d\varphi_r \quad (21)$$

Using the same method and after calculation and simplification, the formula providing the self inductance of the rotor loop can be given as:

$$(L_{rj})_{de} = (L_{rj})_{de1} + (L_{rj})_{de2} \quad (22)$$

where :

$$(L_{rj})_{de1} = \frac{4.\mu_0.r.L}{\pi.\varepsilon_0.\sqrt{1-\delta_d^2}}\sum_{n=1}^{\infty}\left(\frac{sin\left(n.\frac{\alpha_r}{2}\right)}{n}\right)^2 = \frac{(L_{rj})_{healthy}}{\sqrt{1-\delta_d^2}} \quad (23)$$

and:

$$(L_{rj})_{de2} = \frac{2.r.L}{\pi}\sum_{n=1}^{\infty}\frac{sin\left(n.\frac{\alpha_r}{2}\right)}{n}.\sum_{k=1}^{\infty}\lambda_k.\left(\frac{sin\left((n-k).\frac{\alpha_r}{2}\right)}{(n-k)} + \frac{sin\left((n+k).\frac{\alpha_r}{2}\right)}{(n+k)}\right) \quad (24)$$

Similarly, the mutual inductance L_{rirj} between any two rotor loops i and j can be deduced by introducing only the phase angle (φ_{rirj}= (j-i).α_r):

$$(L_{rirj})_{de} = ((L_{ri})_{de1} + (L_{ri})_{de2}).cos(n.\varphi_{rirj}) \quad (25)$$

In presence of dynamic eccentricity, self and mutual inductances of rotor loops are independent of the rotor

position. Hence, these inductances should be calculated only once outside of the iterative process.

3.3. Mutual inductances between stator phases and rotor loops

For a machine with uniform air gap, the mutual inductances between stator phases and rotor loops L_{sr} are similar to the mutual inductances between rotor loops and stator phases L_{rs}. In this section, it will show that, in the case of dynamic eccentricity, the air gap is nonuniform and these mutual inductances will be different. This important result is also confirmed by [6, 13]. The mutual inductance between any stator phase *i* and any rotor loop *j* is the ratio between the flux linked to the rotor loop which is generated by the stator phase and the current following this phase. Hence, the expression of this mutual inductance can be calculated by:

$$\left(L_{sirj}\right)_{de} = r.L.\int_{-\frac{\alpha_r}{2}}^{\frac{\alpha_r}{2}} F_s(\varphi-\varphi_{sisj}).\lambda(\varphi,\theta_r).d\varphi \qquad (26)$$

After calculation of this integral and simplification using trigonometric relations, the mutual inductance between stator and rotor can be expressed by:

$$\left(L_{sirj}\right)_{de} = \left(L_{sirj}\right)_{del} + \left(L_{sirj}\right)_{de2} \qquad (27)$$

where :

$$\left(L_{sirj}\right)_{del} = \frac{L_{sr0}}{\sqrt{1-\delta_d^2}}.\left(\sum_{n=1}^{\infty}\left(\frac{K_b(n)}{n^2}\right).sin\left(n.p.\frac{\alpha_r}{2}\right)cos\left(n.p.\varphi_{sirj}\right)\right) = \frac{\left(L_{sirj}\right)_{healthy}}{\sqrt{1-\delta_d^2}} \qquad (28)$$

φ_{sisj} is the phase angle between the stator phase and the rotor loop, it can be given by :

$$\varphi_{sirj} = \theta_r + (j-1).\frac{2.\pi}{N_r} - (i-1).\frac{2.\pi}{3.p} \qquad (29)$$

and :

$$L_{sr0} = \frac{4.\mu_0.r.L.N_{sp}}{\pi.p^2.\varepsilon_0} \qquad (30)$$

the second term of (27) is given by (31)

Similarly, the mutual inductance between the rotor loop and the stator phase L_{rs} is the ratio between the flux linked to the stator phase which is generated by the rotor loop and the current following this loop. Hence, its expression can be given by:

$$\left(L_{rjsi}\right)_{de} = r.L.\int_{\beta_1}^{\beta_2} F_r(\varphi-\varphi_{sjsi}).\lambda(\varphi).d\varphi \qquad (32)$$

where β_1 and β_2 are given by (12) and φ_{rjsi}=-φ_{sisj}. Hence, the mutual inductance L_{rjsi} can be given by:

$$\left(L_{rjsi}\right)_{de} = \left(L_{rjsi}\right)_{del} + \left(L_{rjsi}\right)_{de2} \qquad (33)$$

where

$$\left(L_{rjsi}\right)_{del} = \frac{\left(L_{sirj}\right)_{healthy}}{\sqrt{1-\delta_d^2}} \qquad (34)$$

and

$$\left(L_{rjsi}\right)_{de2} = \frac{2.r.L.N_{sp}}{\pi.p}.\sum_{n=1}^{\infty}\frac{sin\left(n.p.\frac{\alpha_r}{2}\right)}{n.p}.cos\left(n.p.\varphi_{rjsi}\right).\sum_{k=1}^{\infty}(A_k+B_k) \qquad (35)$$

The expressions show that stator phase–rotor loop mutual inductance and rotor loop-stator phase are dependent on the rotor position. A comparison is shown in figure 2 between the mutual inductance of the first stator phase and the first rotor loop for a healthy machine and for a machine with 50% of dynamic eccentricity. This figure shows also the mutual inductance between the first rotor loop and the first stator phase. It is obvious that the mutual inductances increase in presence of dynamic eccentricity and the mutual inductance between stator phases and rotor loops are different from the mutual inductances between the rotor loops and the stator phases Figure 3 shows the curves of mutual inductances between stator phases and the rotor loops. It is obvious that the value of the mutual inductance declines with the rise of the air gap length. Mutual inductances between the rotor loops and the stator phases are illustrated in figure 4.

It can be noted that the shapes of these curves are similar to that of the stator-rotor mutual inductances in a symmetrical machine. Only the magnitude increases with the dynamic eccentricity. This is due to the fact that the rotor loop in a standard cage rotor induction machine has a quite small pitch, so the rotor loop in one position of the rotor does not experience a significant change in air gap length

$$\left(L_{sirj}\right)_{de2} = \frac{2.N_{sp}.r.L}{\pi.p}.\sum_{n=1}^{\infty}\frac{K_b(n.p)}{n}.\sum_{k=1}^{\infty}\lambda_k.\left(\frac{sin\left((n.p+k).\frac{\alpha_r}{2}\right).cos\left(k.\theta_r+n.p.\varphi_{sirj}\right)}{(n.p+k)} + \frac{sin\left((n.p-k).\frac{\alpha_r}{2}\right).cos\left(k.\theta_r-n.p.\varphi_{sirj}\right)}{(n.p-k)}\right) \qquad (31)$$

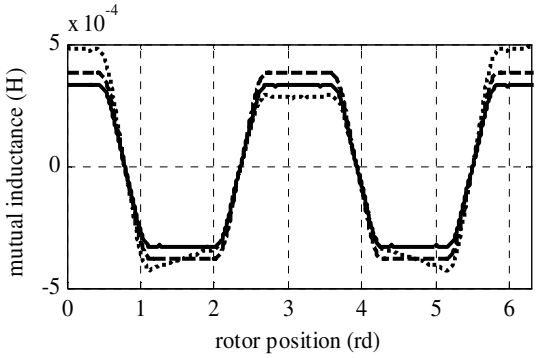

Fig. 2. Comparison between mutual inductances

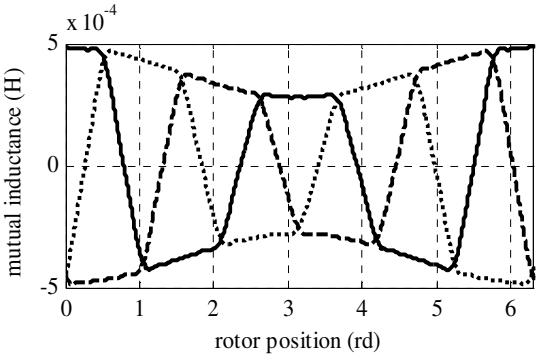

Fig. 3 Mutual inductance between the three stator phases and the first rotor loop,

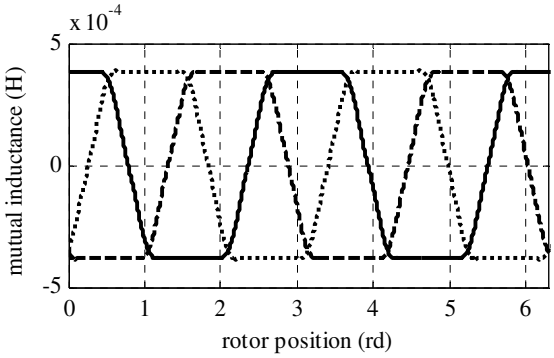

Fig. 4 Mutual inductance between the rotor and the first rotor loop and the three stator

4.Simulation results

The developed model is used to simulate a squirrel cage induction machine in the case of healthy and faulty conditions. For this purpose, a computer script written in MATLAB/SIMULIK has been developed. First it is assumed that the machine is supplied by three-phase sinusoidal voltages. Figure 5 illustrates the rotor speed in case of a healthy and a faulty machine with δ_d=0.2, 0.4 and 0.6 with a load torque of 10 N.m. Under these conditions, the slip is 8.6% for the healthy machine and for the faulty one with δ_d=0.2 and δ_d=0.4. For the case of δ_d=0.6 the slip is 8.2%. It can be noted that the acceleration time under dynamic eccentricity is larger than under healthy case. This can be explained by the additional reluctant torque component that

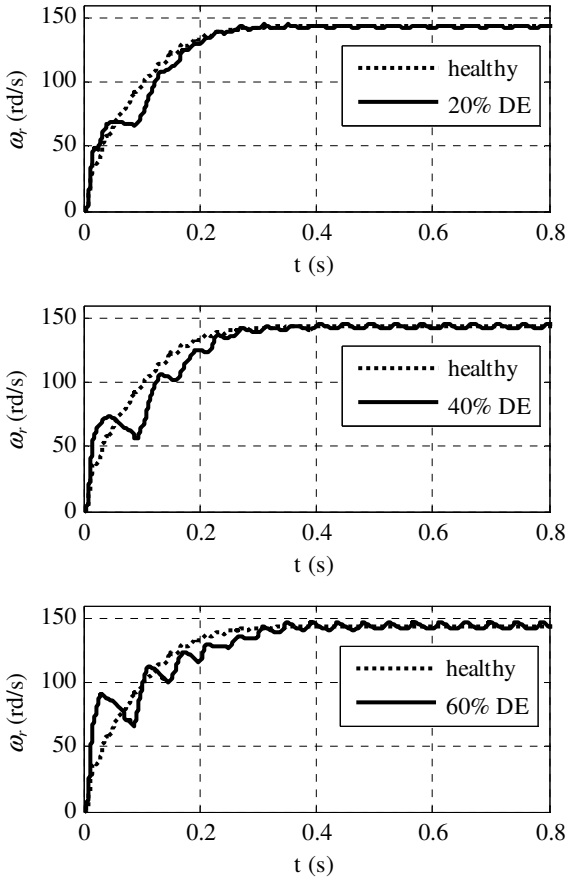

Fig. 5 Rotor speed

compensates for the inherently smaller induction torque component due to the higher air gap length along the main part of machine circumference. Figure 6 presents the stator currents for both healthy and faulty cases. As shown in the theoretical analysis, in presence of dynamic eccentricity, the stator currents magnitude is modulated and this modulation increase with the fault severity. Figure 7 demonstrates the steady state stator current spectrum in the interval [0 100 Hz] for the healthy and the faulty cases under different dynamic eccentricity degrees. The spectrum is obtained by the estimation of Power Spectral Density PSD using Welch technique with Hanning window. As predicted by the theoretical analysis presented in [14-16], this figure shows clearly that components with frequencies $f_s \pm n.f_r$| are present around the fundamental component for machines with dynamic eccentricity. The amplitude of these components increases with the fault severity. For n=1, Lower Sideband Component LSB with frequency (f_s-f_r) increases from -17.36 dB for δ_d=0.2 to -12.14 dB and -8 dB for δ_d=0.4 and δ_d=0.6 respectively. However, for the Upper Sideband Component USB with frequency (f_s+f_r), there is a difference of 4.65 dB between the amplitude of this component for δ_d=0.2 and δ_d=0.4. This difference is 3.38 dB when the degree of dynamic eccentricity increases from δ_d=0.4 to δ_d=0.6.

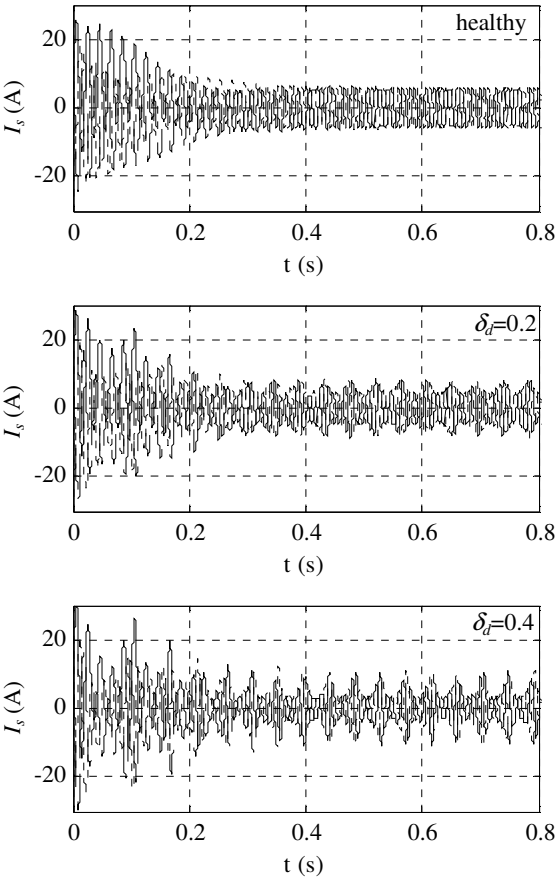

Fig. 6 Stator currents

Figure 8 shows the steady state stator current spectrum in the interval [500 800Hz] for machine with 40% of dynamic eccentricity operating under 10 N.m load torque. The Principal Slots Harmonics PSH can be located in this spectrum. As indicated in the theoretical analysis, the frequency of these components corresponds exactly to this given by:

$$PSH = \left(\frac{k.N_r}{p}(1-g) \pm \nu \right).f_s \qquad (36)$$

The frequency of the first component is 588.5 Hz and for the second one is 688.5 Hz. However, other components exist around the slots harmonics due to the dynamic eccentricity. The frequency of these harmonics is given by (37) and can be indicated in figure 8.

$$f_{ed} = \left((k.N_r \pm n).\frac{(1-g)}{p} \pm \nu \right).f_s \qquad (37)$$

In order to analyse the effect of time harmonic on the spectrum of the stator current, the proposed model is also used to simulate the induction machine with dynamic eccentricity when the supply is a sinusoidal PWM voltage source inverter

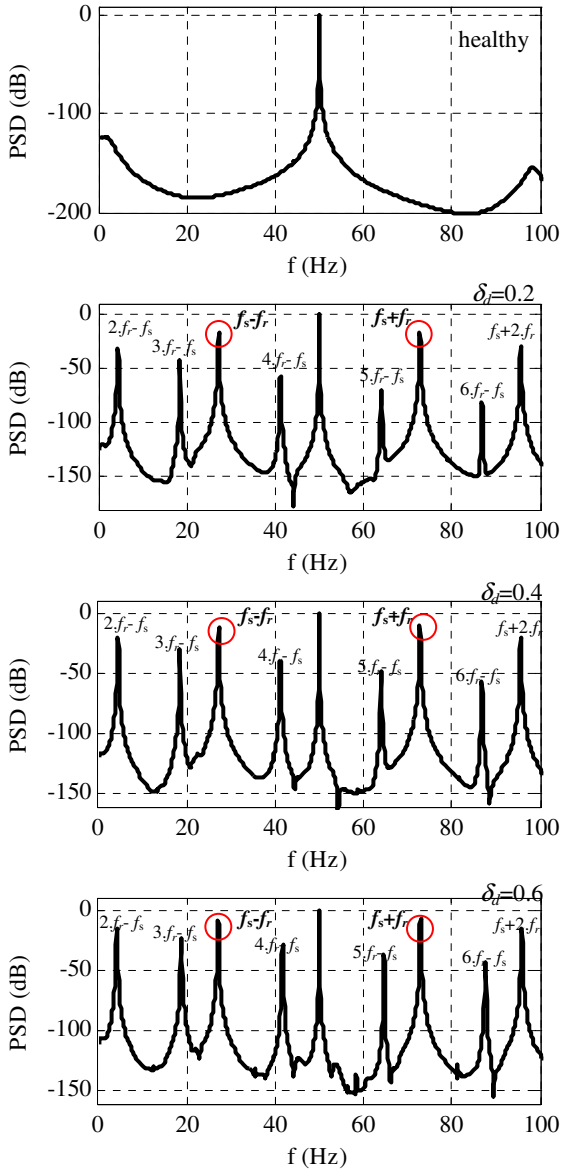

Fig. 7. Stator current spectra around the fundamental,

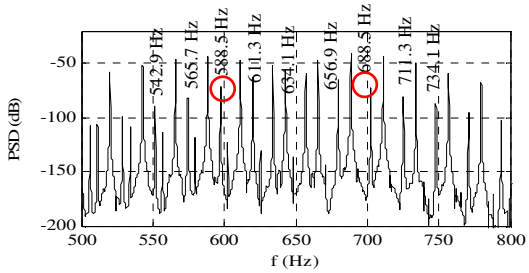

Fig. 8. Stator current spectra around the PSH for machine supplied by sinusoidal voltages with δd=0.4

The output voltage of the inverter contains in addition to the fundamental, other components with frequency $(m.k_1 \pm k_2).f_s$ where m is the modulation index, (k_1, k_2) are integer and (k_1+k_2) an odd integer [17].

Figure 9 shows the stator current spectrum around the fundamental for δ_d=0.4. Compared to the spectrum of Figure 7-c, the spectrum showed by this figure contains in addition to the specific fault harmonics with frequency $|f_s \pm n.f_r|$, other components with small amplitude due to the PWM harmonics.

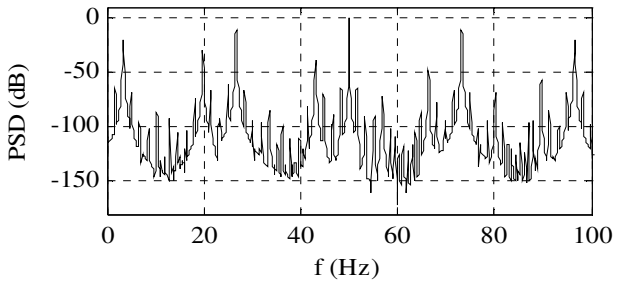

Fig. 9 Stator current spectra around the fundamental for machine supplied by PWM inverter with δd=0.4

6. Conclusion

In this paper, the analytical expressions of the self and mutual inductances of the induction machine in presence of dynamic eccentricity are presented. These inductances are obtained using the magnetomotive force and the airgap permeance approach including the space harmonics effect. The magnitude of these inductances increases with the dynamic eccentricity degree compared to a healthy machine. In addition of this, the self and mutual inductance of the stator become variable with the rotor position. Concerning the mutual inductances between the stator and the rotor, the results obtained with this approach confirm that the mutual inductances of the stator-rotor loops are different from the mutual inductances of the rotor-stator phases. The developed inductances are introduced in a general model of an induction machine obtained using the magnetically coupled circuits approach. Simulations are performed for two different voltage supplies. The first one is a perfect sinusoidal supply whilst the second one is a PWM voltage inverter. The Power Spectral Density of the stator current is used to detect the specific components of the dynamic eccentricity fault. It has been shown that in case of PWM supply, the identification of these components is more difficult than for a sinusoidal supply.

References

1 A. H. Bonnett 'Root Cause AC Motor Failure Analysis with a Focus on Shaft Failures' *IEEE Transactions on Industry Applications*, Vol. 36, N° 5, September/October 2000.

2 W. T. Thomson, D. Rankin, and D. G. Dorrell, "On-line current monitoring to diagnose airgap eccentricity in large three-phase induction motors-industrial case histories verify the predictions," *IEEE Trans. on Energy Conversion*, Vol. 14, N° 4, pp1372-1378, Dec. 1999.

3 W. T. Thomson, D. Rankin, and D. G. Dorrell, "On-line current monitoring to diagnose airgap eccentricity-an industrial case history of a large high-voltage three-phase induction motors," *Electric Machines and Drives Conference Record*, ppMA2/4.1-MA2/4.3, 1997.

4 W. T. Thomson and A. Barbour, "The on-line prediction of airgap eccentricity levels in large (MW range) 3-phase induction motors," *IEEE International Electric Machines and Drives Conference,* pp383-385, 1999.

5 M. Sahraoui, A. Ghoggal, S.E. Zouzou and M.E. Benbouzid, "Dynamic eccentricity in squirrel cage induction motors – Simulation and analytical study of its spectral signatures on stator currents," *Simulation Modelling Practice and Theory, Elsevier,* pp. 1-11, August 2008.

6 H. A. Toliyat, M. S. Arefeen and A. G. Parlos, "A method for dynamic simulation of air-gap eccentricity in induction machines," *IEEE Trans. Ind. Appl.*, Vol. 32, N°4, pp. 910-918, July/August 1996.

7 J. Faiz and I. Tabatabaei, "Extension of Winding Function Theory for Nonuniform Air Gap in Electric Machinery," *IEEE Trans. on Magnetics*, Vol. 38, N° 6, pp. 3654- 3657, Nov. 2002

8 G. Bossion, C. D. Angelo. J. Solsona and M. I. Valla,"A 2D-model of the induction motor: an extension of the modified winding function approch," *IEEE Trans. On Energy Conv.,* Vol. 19, N° 1, pp. 144- 150, March 2004

9 A. Ghoggal, S.E. Zouzou, H. Razik, M. Sahraoui and A. Khezzar, "An improved model of induction motors for diagnosis purposes – Slot skewing effect and air–gap eccentricity faults," journal of Energy Conversion and Management N° 50, pp. 1336–1347, 2009

10 J. Faiz, B. M. Ebrahimi, M. Valavi et H. A. Toliyat, "mixed eccentricity fault diagnosis in salient-pole synchronous generator using modified winding function method," Progress In Electromagnetics Research B, Vol. 11, pp.155–172, 2009

11 H. Akbari, "analytical computation of reluctance synchronous machine inductances under different eccentricity faults," Progress In Electromagnetics Research M, Vol. 24, pp. 29-44, 2012

12 S. Hamdani, O. Touhami et R. Ibtiouen, "A generalized two axes model of squirrel-cage induction motor for rotor faults diagnosis," *Serbian Journal of Electrical Engineering SJEE*, Vol. 5, N°1, pp. 155-170, Mai 2008.

13 G. M. Joksimovic, M. D. Durovic, J. Penman and N. Arthur, "Dynamic Simulation of Dynamic Eccentricity in Induction Machines-Winding Function Approach," *IEEE Transactions on Energy Conversion*, Vol. 15, No. 2, pp 143-148, June 2000.

14 H. Henao, C. Martis and G. A. Capolino, "An Equivalent Internal Circuit of the Induction Machine for Advanced Spectral Analysis," *IEEE Trans. Ind. Appl.*, Vol. 40, N°3, pp. 726-734, May/June 2004.

15 X. Li, Q. Wu and S. Nandi, " Performance Analysis of a Three-Phase Induction Machine With Inclined Static Eccentricity," *IEEE Trans. Ind. Appl.*, Vol. 43, N°2, pp. 531-541, Mar./Apl. 2007.

16 H. Guldemir, "Detection of airgap eccentricity using line current spectrum of induction motors," *Electric Power Systems Research, Elsevier* pp. 109- 117, 2003.

17 B. K. Bose, "Modern power electronics and AC drives," Prentice Hall PTR, pp. 211- 214.